

Physical properties and orbital stability of the Trojan asteroids

Melita, M.D.¹

and

Licandro, J.²

and

Jones, D.C.³

and

Williams, I.P.³

¹ IAFE (UBA, CONICET) Argentina. melita@iafe.uba.ar

² Isaac Newton Group of Telescopes, La Palma, Spain

and

Instituto de Astrofísica de Canarias, Tenerife, Spain.

³ Astronomy Unit, Queen Mary College, University of London, UK.

Received _____; accepted _____

Submitted to *Icarus*

ABSTRACT

All the Trojan asteroids orbit about the Sun at roughly the same heliocentric distance as Jupiter. Differences in the observed visible reflection spectra range from neutral to red, with no ultra-red objects found so far. Given that the Trojan asteroids are collisionally evolved, a certain degree of variability is expected. Additionally, cosmic radiation and sublimation are important factors in modifying icy surfaces even at those large heliocentric distances.

We search for correlations between physical and dynamical properties, we explore relationships between the following four quantities; the normalised visible reflectivity indexes (S'), the absolute magnitudes, the observed albedos and the orbital stability of the Trojans.

We present here visible spectroscopic spectra of 25 Trojans. This new data increase by a factor of about 5 the size of the sample of visible spectra of Jupiter Trojans on unstable orbits. The observations were carried out at the ESO-NTT telescope (3.5m) at La Silla, Chile, the ING-WHT (4.2m) and NOT (2.5m) at Roque de los Muchachos observatory, La Palma, Spain.

We have found a correlation between the size distribution and the orbital stability. The absolute-magnitude distribution of the Trojans in stable orbits is found to be bimodal, while the one of the unstable orbits is unimodal, with a slope similar to that of the small stable Trojans. This supports the hypothesis that the unstable objects are mainly byproducts of physical collisions.

The values of S' of both the stable and the unstable Trojans are uniformly distributed over a wide range, from 0 %/1000Å to about 15 %/1000Å. The values for the stable Trojans tend to be slightly redder than the unstable ones, but no significant statistical difference is found.

Subject headings: ASTEROIDS, DYNAMICS; ASTEROIDS, COMPOSITION;
COMETS

1. Introduction

The main motivation of this work is to look for correlations between physical and dynamical properties. We shall discuss ways in which the diversity in surface properties can develop, how relationships with orbital stability may originate and what this may imply.

The Trojan asteroids are believed to have been formed in the outer Solar System (see for example Marzari & Scholl 1998 or Morbidelli *et al.* 2005) so, ices may be expected to be their main component. However, at the moment, no water or other more volatile substances have been detected on the surface of a Trojan (Yang & Jewitt 2007, Emery & Brown 2003, Emery & Brown 2004). Infrared observations indicate the presence of silicates (Cruikshank *et al.* 2001, Emery *et al.* 2006). In the case of Ennomos, an unusually high-albedo object, the surface-content of water ice has been quantified to be below 10% in mass (Yang & Jewitt 2007).

Cosmic Radiation modifies the spectroscopic properties of these types of compounds. The precise effect depends on the chemical composition of the asteroidal surface, that of the incoming cosmic radiation and its energy. Laboratory experiments of ion-radiation, of energies in the order of keV, gradually ‘flattens’ the spectral slopes of organic-complexes such as asphaltite and kerite (Moroz *et al.* 2004), while it produces red and dark residuals upon ice-surfaces such as methanol, methane and benzene, turning the spectra to neutral for very high doses (Brunetto *et al.* 2006a). Micrometeorite bombardment also lowers the albedo and reddens the surface of silicates rich in olivine, pyroxene and serpentine, as indicated by experiments using UV-laser pulses which simulate this effect (Brunetto *et al.* 2006b); the corresponding timescale to modify the spectral slope on main belt asteroids are estimated to range between 10^8 yr to 10^{10} yr. On the other hand, experiments of ion-irradiation on a sample of the meteorite Epinal indicate that this timescale for an S-type asteroid could be as short as 10^4 yr to 10^6 yr in the NEA population (Strazzulla *et al.*

2005). The timescale in which the surface spectral properties of asteroids will be modified in the Jupiter region is not simple to estimate as it depends on the modulation of the solar activity at these distances. But, since the density of the cosmic radiation originated in the Sun decreases as the heliocentric-distance squared, one may argue that, if any of these processes is relevant for the Trojans, these timescales should be increased by at least an order of magnitude.

The abundance of irradiated material decreases with depth, hence, if material originally from the interior is exposed in some objects, color differences would emerge between members of the same population. Collisions between objects is an obvious way of achieving this and, according to Dell’Oro *et al.* (1998), collisions can be significant in the Trojan population. In the trans-Neptunian population, Gil-Hutton (2002) has shown that links between surface and orbital properties can be established in this way.

Although the Trojan asteroids are located at a large heliocentric distance, ice sublimation could also be an important factor affecting their surfaces. A thin insulator mantle can form in a very short timescale that ranges from 10^4 yr to 10^6 yr (Jewitt 2002).

There is a slow dynamical evaporation of bodies from the Trojan clouds due to gravitational perturbations, with the 5 : 2 mean motion resonance with Saturn being very important (Levison *et al.* 1997, Nesvorný & Dones 2002, Tsiganis *et al.* 2005). In particular, Thersites (1868), has a high probability of leaving the Trojan swarm in less than $50Myr$ (Tsiganis *et al.* 2000). But the out-flux rate produced by collisions is much larger. Marzari *et al.* (1995) have found that there is an out-flux of one Trojan asteroid greater than $1km$ in size every $1000yr$. The smaller byproducts of a collision are more numerous and tend to have greater post-encounter velocities and are thus less likely to remain in the most stable regions. Hence, collisions could create variability in surface properties and at the same time produce a correlation between physical properties and dynamical state.

Within the Trojan Clouds there exist a number of dynamical families, which are believed to have been formed collisionally. Fornasier *et al.* (2004), Fornasier *et al.* (2007) and Dotto *et al.* (2006) found that, for a given family, there is a similarity in the surface properties of the members, except for a few objects that are physically different and these have been called *interlopers*. Unfortunately, the information regarding the surfaces of Trojan asteroids that belong to families is rather sparse to date.

It must also be noticed that interloper objects such as captured comets might exist in the Trojan clouds (Rabe 1972, Yoder 1979). Indeed, objects in Centaur-type orbits are known to evolve into temporary Trojans for time-spans of some 0.5 Myr (Horner *et al.* 2005) and ‘transitional’ objects with orbits that can evolve into short period comets are known to exist in the 1 : 1 resonance with Jupiter (Karlsonn 2004).

Up to now, it was not possible to investigate correlations between dynamical stability and spectroscopic properties because the colors of the transitional Trojans were largely unknown. In order to rectify this, we have obtained new low-resolution visible spectra of an additional 24 Trojans in unstable orbits.

This article is organised as follows. In section 2 we discuss the methods used to study the dynamical properties of the Trojan asteroids. We present the data used in this study in section 3, both the observations carried out for the purpose of this investigation and also the data taken from other authors. Correlations between physical and dynamical properties are discussed in section 4. Finally, in section 5, we discuss our results

2. Determination of dynamical properties

In order to discuss whether a Trojan is in a primordial orbit or subject to a recent perturbation we need to know the time that it can remain on or near its present orbit.

Variations in the proper elements of the orbits can occur as a result of physical collisions. As a consequence of this random walk in phase space, the asteroid may find an unstable regime, leading to the expulsion from the Trojan Cloud in a timescale that is smaller than the age of the Solar System –i.e. its present life as a Trojan is only a ‘transitional’ phase. If some asteroids exist in those transitional orbits today, we may conclude that they are likely to have been inserted there recently, most probably because of collisions (Marzari *et al.* 1995).

The best way of determining the residence lifetime is to numerically integrate the equations of motion of each asteroid over the age of the Solar System. However, even with efficient integrators, this is a very large task. For this reason, we have explored the accuracy of a chaos estimator, the Lyapunov Characteristic Exponent (LCE) when applied to estimating macroscopic stability of the orbits of known Trojan asteroids. The *LCE* gives the rate of exponential divergence from perturbed initial conditions, given $X_0(t)$, a point in the orbit of the unperturbed problem, if we can write $X(t) = X_0(t) + U(t)$, where $X(t)$ is the perturbed solution and $U(t)$ is the deviation from the unperturbed trajectory at time t , the *LCE* is defined as:

$$LCE = \lim_{t \rightarrow \infty} \frac{1}{t} \ln|U(t)|.$$

Naturally, we do not expect the *LCE* to be 100% reliable as an estimator of macroscopic stability, because some orbits can be in a ‘stable-chaos’ regime (Milani and Nobili 1992, Milani 1993, Milani *et al.* 1997), which may render both a high value of *LCE* and a long lifetime as a Trojan (Pilat-Lohinger and Dvorack 1999, Dvorack and Tsiganis 2000).

In order to test the applicability of *LCE*, we integrated the equations of motion of the orbits of 32 Trojan asteroids, using Mercury 6 (Chambers 1999), taking into account the gravitational interactions of the Sun, Jupiter and Saturn. The numerical integration of the orbit is terminated when the asteroid ceases to co-orbit with Jupiter, defined to be

when the semi-major axis moves $0.4AU$ away from the semi-major axis of the planet. All the integrations were performed for at least $3.06Gy$. The objects selected for the dynamical study belong to our sample of available visible spectra and include all the 24 objects observed by us.

Our results are summarised in table 1. We conclude that all objects with $LCE < 0.53 \times 1/(10^5yr)$ are macroscopically stable and most objects with $LCE > 0.7 \times 1/(10^5yr)$ are unstable, but a few (22%) may have found islands of stability, most of them with exponents in the range $0.7 \times 1/(10^5yr) < LCE < 1.0 \times 1/(10^5yr)$, which agrees well with previous stability studies (Tsiganis *et al.* 2005).

We conclude that, for our purposes, the use of LCE is adequate to determine statistically the macroscopic stability of the Trojan asteroids, but we must bear in mind that there is a small ‘contamination’ of the population deemed by the LCE to be unstable that are in fact stable.

3. Visible Spectra of Trojan asteroids

To obtain as wide a data-base as possible on the spectra of Trojan asteroids, we have used both data from our own observational program and published data from a number of other sources.

3.1. New Observations

To obtain results with the best possible statistical significance, we performed our observations at a wavelength where the existing data is the most abundant, which is, naturally, the visible range. Our sample, as mentioned earlier, deliberately consists mainly

of transitional objects. All objects in the dynamical study were included in the observing sample.

Visible spectra were obtained with the 3.5m New Technology Telescope (NTT), at ESO La Silla (Chile), the 4.2m William Herschel (WHT) and the 2.5 m Nordic Optical Telescope (NOT) both at the “Roque de los Muchachos” Observatory (ORM, La Palma, Spain).

At NTT the RILD arm of EMMI with the grism#7 (150gr/mm) was used, covering the 5200 – 9300Å spectral range, with a dispersion of 3.6Å/pix. Spectra were taken through a 5 arcsec wide slit. Observational circumstances for NTT observations are shown in tables 2.

At the WHT the red red arm of ISIS spectrograph with the R158R grating (158gr/mm) centred at 7500Å and a second order blocking filter that cut at 0.495 μm was used, covering the 5000 – 9500Å spectral range, with a dispersion of 1.63Å/pixel. Spectra were taken through a 5arcsec wide slit. Observational circumstances for WHT observations are shown in table 3.

At the NOT the ALFOSC (Andalucia Faint Object Spectrograph and Camera) with a grism disperser #4 (300gr/mm) and GG475 second order blocking filter was used, covering the 4800 – 9100Å spectral range, with a dispersion of 3Å/pixel. Spectra were taken through a 1.3 arcsec wide slit. Observational circumstances for NOT observations are shown in table 4.

In all telescopes the slit was oriented in the parallactic angle, and the tracking was at the asteroid proper motion.

Data reduction was carried out in the standard way using standard IRAF procedures. Images were over-scan and bias corrected, and flat-field corrected using lamp flats. The two-dimensional spectra were extracted, sky background subtracted, and collapsed to one dimension. The wavelength calibration was done using Helium, Neon and Argon

lamps. The reflectance spectra were obtained by dividing the spectra of the asteroids by the spectra of Solar-analogue star Hyades 64 and G2 stars Landolt 98-978 and Landolt 102-1081 (Landolt, 1992), observed during the same night at airmasses similar to that of the asteroids. Reflectance spectra, normalised at $0.6 \mu\text{m}$, are shown in figures 1, 2 and 3.

We characterise the color of the surfaces by the reflectivity gradient, S' , in the wavelength interval $[5100\text{\AA} - 7400\text{\AA}]$, where:

$$S' = 1/S(6000\text{\AA}) \frac{\Delta S}{\Delta \lambda},$$

S is the normalised reflectivity with respect to a Solar-analogue star and λ , the wavelength. We have chosen a wavelength range where we have data from all the available observations.

The value of S' , computed in that wavelength range, gives a good estimation of the nature of the surface. Most Trojans are quite red objects and have been classified as D -types or P -types (see for example Bendjoya *et al.* 2004), which means that their spectra are featureless and linear, with a positive slope.

The obtained values of S' for our own group of targets are given in table 5, where we also give the corresponding value of LCE and the absolute magnitudes, H , taken from the *AstDys* database¹.

3.2. Spectral information from other published databases

The data used in this work were taken from : Jewitt & Luu (1990) (32 observations Ref id: 1), SMASSII (Bus, 1999, 5 observations, Ref id: 2), Bendjoya *et al.* (2004) (34 observations, Ref id: 3), Lazzaro *et al.* (2004) (10 observations, Ref id: 4), Dotto *et al.* (2006

¹<http://hamilton.dm.unipi.it/cgi-bin/astdys/astibo>

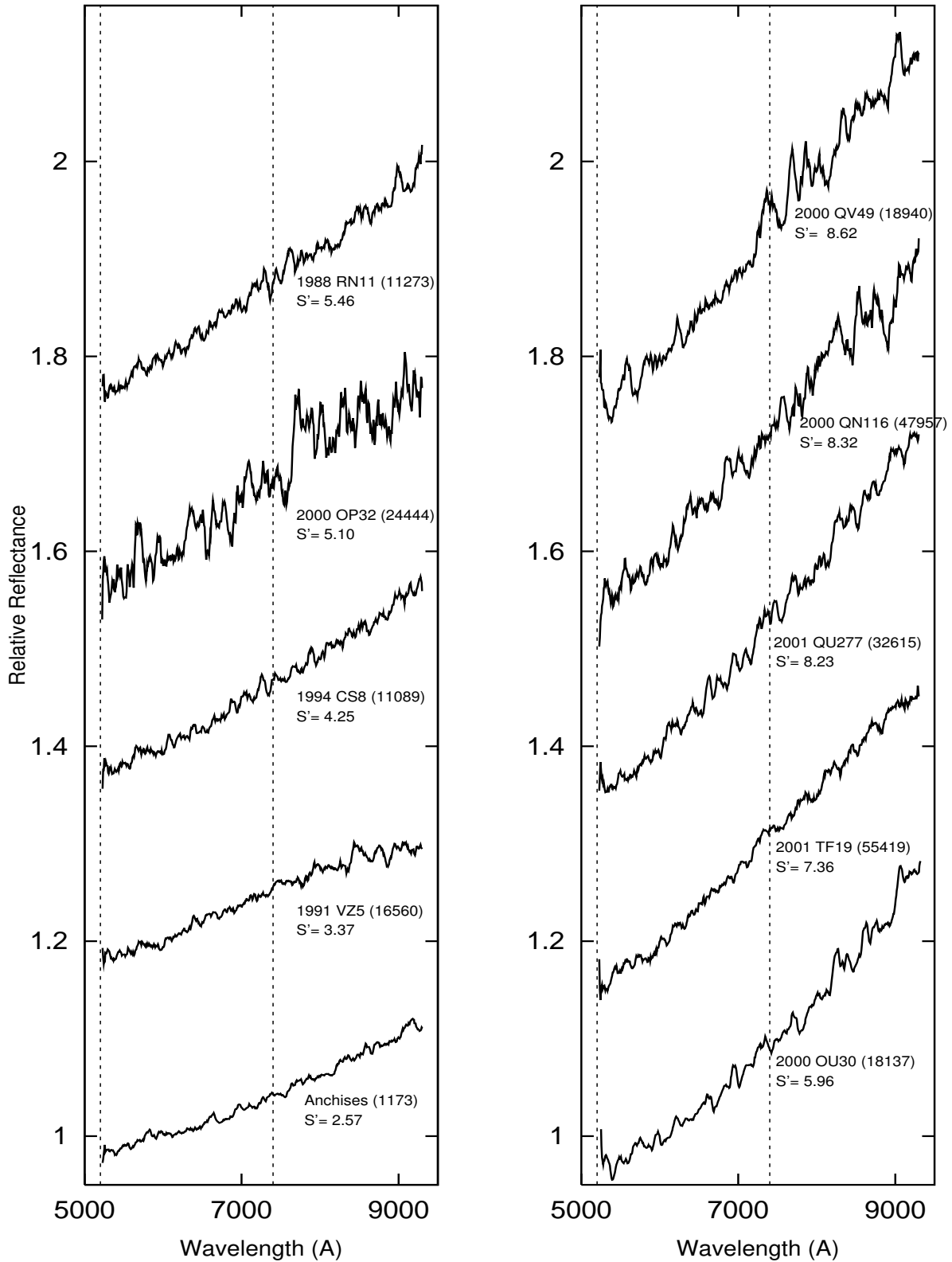


Fig. 1.— Spectra of the 10 Trojan asteroids observed at NTT-ESO. The relative reflectance is shifted vertically by an additive constant for clarity. The vertical dotted lines indicate the range over which the linear fit has been made.

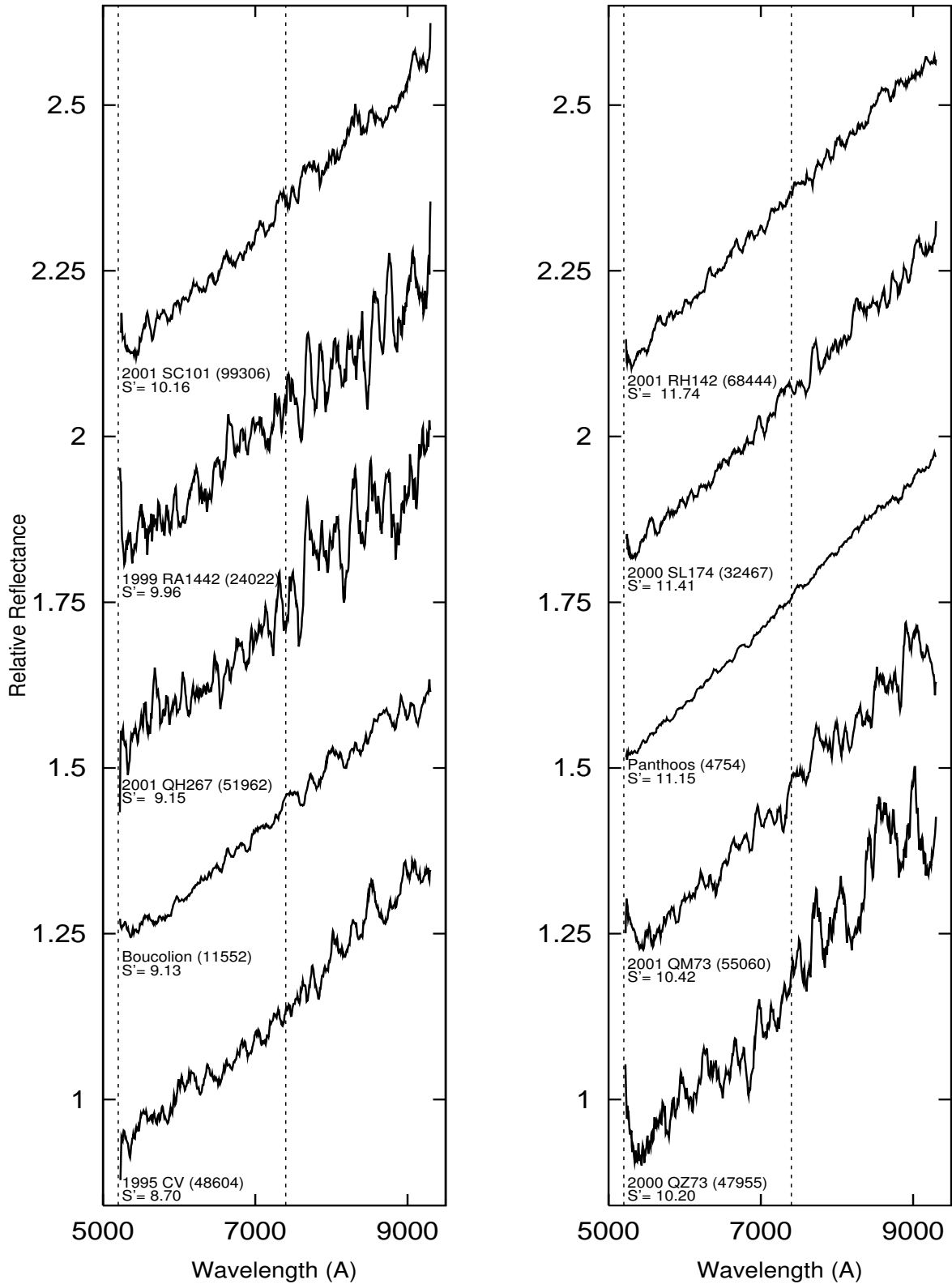


Fig. 2.— Spectra of the 10 Trojan asteroids observed at NTT-ESO (cont.). The relative reflectance is again shifted by an additive constant for clarity. The vertical dotted lines indicate the range over which the linear fit has been made.

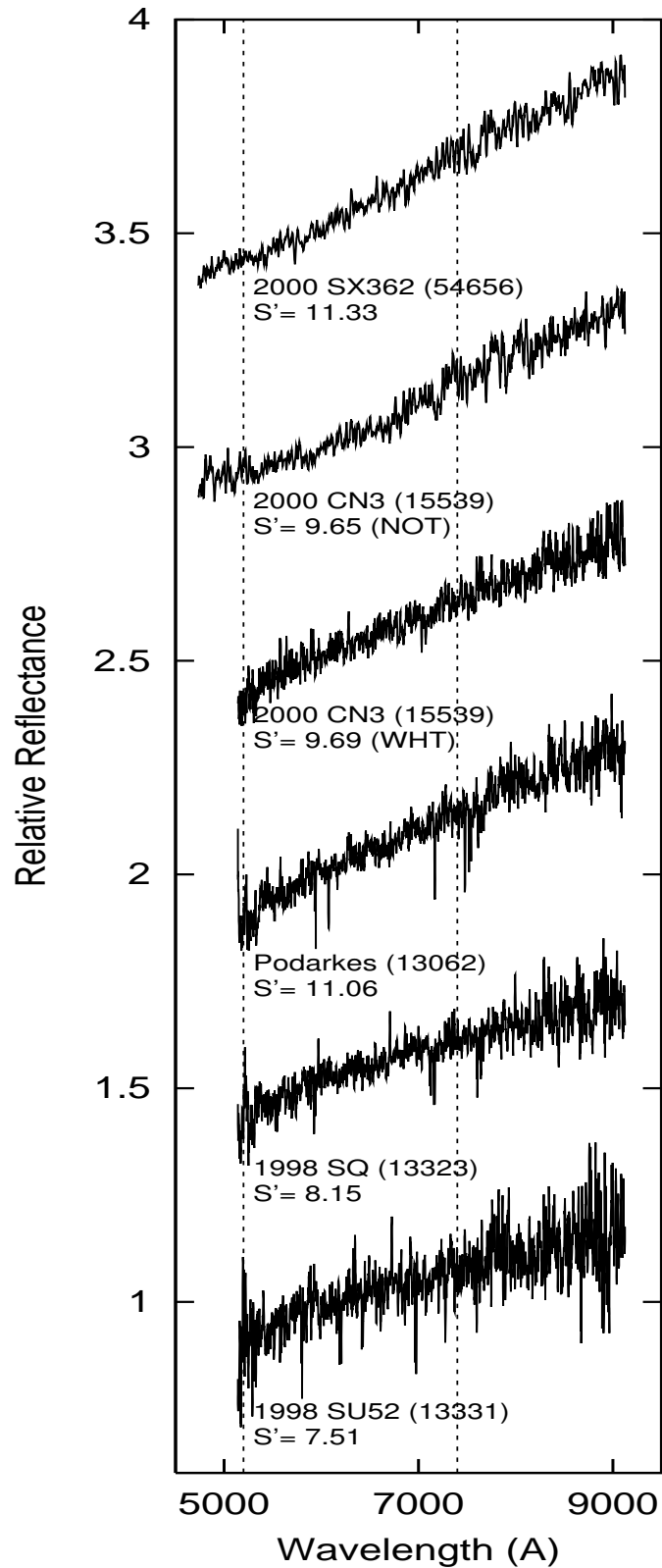


Fig. 3.— Spectra of the 5 Trojan asteroids observed at WHT-ING and NOT. The relative reflectance is again shifted by an additive constant for clarity. The vertical dotted lines indicate the range over which the linear fit has been made.

Ref id: 5)² (5 observations). The data from Fornasier et al (2007) is not available to us. Their sample is composed of 47 objects, all family members, whose surface properties may not statistically mimic those of the whole Trojan population so they may have introduced an unwanted bias.

We have computed the value of S' by a linear fit in the [5100Å – 7400Å] wavelength range for the spectra found in the databases of Bus (1999) and Lazzaro *et al.* (2004). The spectra from Jewitt and Luu (1990) was scanned to compute the value of S' in that same interval. For the article of Bendjoya *et al.* (2004) we used the quoted value of S' , since the interval is very similar to the one chosen by us. All the correspondent values are listed in tables 6, 7 and 8.

3.3. Differences between the various data sets

In all we have a total of 112 observations corresponding to 96 different objects. There are 15 objects that have S' determined from two sources observations and two from three sources.

In table 9 we have listed the objects that have repeated observations. The median value of the differences in the values of S' for the repeated observations, $\langle \Delta S' \rangle_{med}$, is:

$$\langle \Delta S' \rangle_{med} \sim 2.5.$$

Based on this, we adopted a value for the typical observation error of S' as $\langle \Delta S' \rangle_{med}$. Those observations with values of S'_d , such that (with $|S'_d - \langle S' \rangle_{med}| > 3 \times \langle \Delta S' \rangle_{med}$) will be discarded from the analyses. Therefore objects with values of $S' \lesssim 0$ and $S' \gtrsim 15$ will not be considered. We exclude from our sample the following objects: 5283 ($S' = -8.9$,

²Only a subset of the spectra contained in this article is available to us.

Ref id.:3), 1870 ($S' = 20.34$, Ref id.:1) and 1872 ($S' = 25.42$, Ref id.:1). Therefore the total number of objects of the sample is 93. For objects with more than one value of S' originating in different sources, we use their mean value.

We also note that the median of differences is much smaller if the objects from Bendoya *et al.* (2004) are excluded, giving: $\langle \Delta S' \rangle_{med} = 0.35$.

4. Correlations between various properties

4.1. Size distributions of the resident and the transitional groups

In this section we compare the size distributions of the resident and the transitional Trojans. If the unstable orbits are mainly fed by the smallest by-products of collisions, the size distributions of the stable and the unstable groups will be different, but if the only mechanism by which a Trojan asteroid reaches an unstable orbit is dynamical, then both the size distributions will be similar.

We assume that the absolute magnitude, H , is a reliable indicator of the size of the asteroids. The absolute magnitudes, H , of the asteroids are taken from *AstDys*. The H -distribution of both groups is shown in figure 4. We considered only multi-opposition objects with $H < 12$, since it is apparent from figure 4 that for fainter objects the sample has additional bias selection effects.

We have divided the numbered Trojan asteroids into 2 groups, according to the value of LCE , such that the *resident* Trojans have $LCE_{res} \leq 0.53 \times 1/(10^5 yr)$ and the *transitional* ones, $LCE_{trans} > 0.53 \times 1/(10^5 yr)$. According to this criteria, in the *AstDys* database we have found 517 resident and 121 transitional multi-opposition Trojans.

Realistic variations in the geometrical albedo, p_V , for values in the range observed in

the Trojan populations, makes little difference to the value of the diameter. Assuming a mean geometrical albedo of $p_V = 0.04$ (Fernandez et al. *et al.* 2003), the objects in our sample have diameters between $20km$ and $260km$ approximately.

As we can see from fig 5, there is a tendency for objects in more unstable orbits to be smaller.

The absolute magnitude distributions of these groups, shown in figure 4, are fit with linear functions of the type:

$$\log_{10}(N) = b H + a.$$

For a bimodal distribution the fit is done between the absolute magnitude distribution and 2 linear-functions:

$$\begin{aligned} \log_{10}(N_1) &= b_1 H + a_1 & H < H_n \\ \log_{10}(N_2) &= b_2 H + a_2 & 12 > H > H_n \end{aligned} \tag{1}$$

We also require that:

$$a_1 + b_1 H_n = a_2 + b_2 H_n.$$

We calculate the corresponding values of χ^2 as a function of H_n . The first and last values of H_n are chosen to include 5 data-points. The nodal point, H_{node} , corresponds to the value of H_n that gives the minimum value of χ^2 (see figure 6). We find that the value of the nodal point for the resident Trojans is $H_{node} = 9.41$.

For the transitional Trojans, the values of χ^2 obtained with the bimodal fit are not significantly different from the one of a single linear fit (see also figure 6).

The value of slopes corresponding to the best fits are shown in table 10. It is apparent that the absolute magnitude distribution of ‘small’ resident Trojans is similar to the one

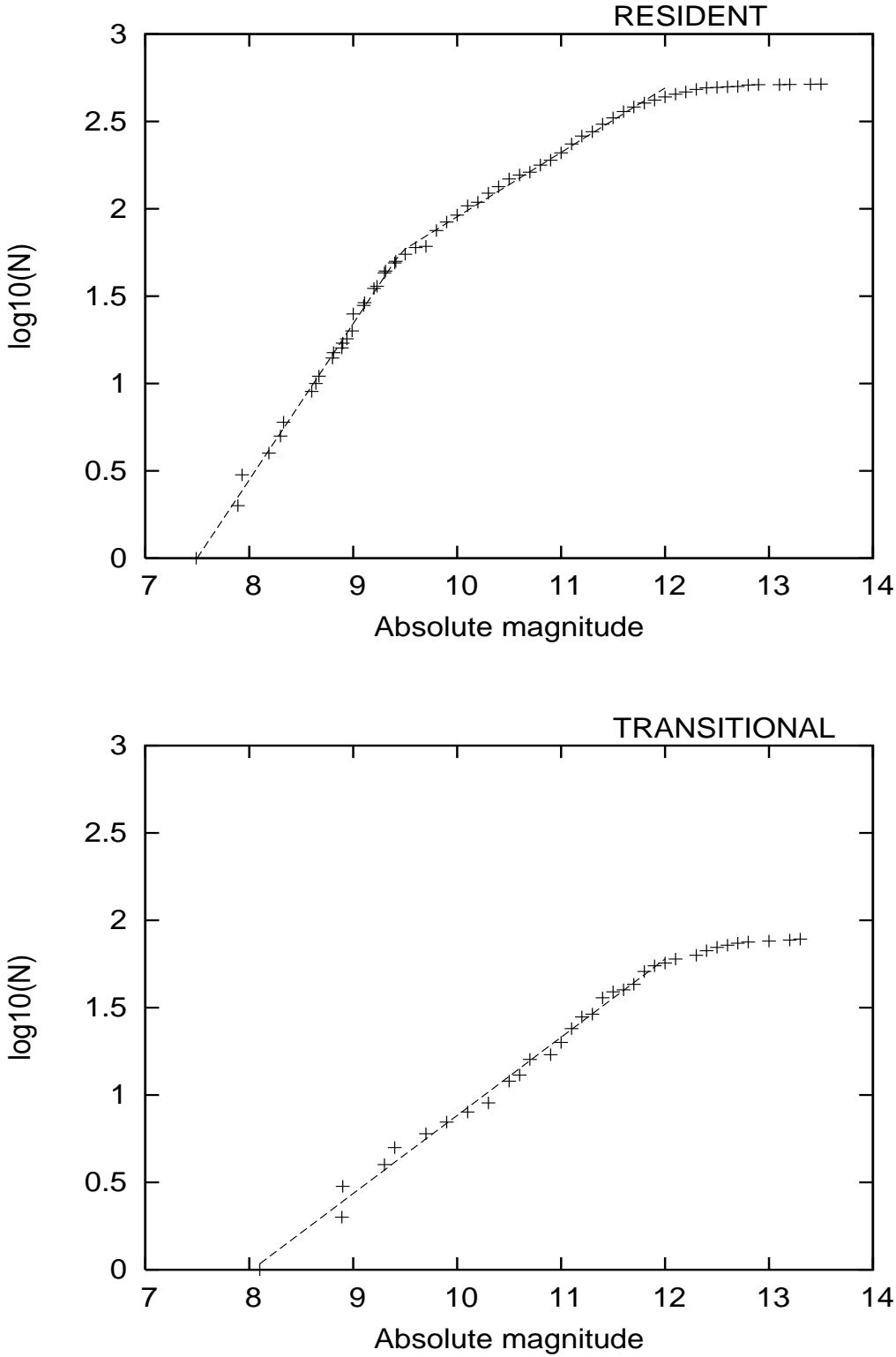


Fig. 4.— Absolute magnitude distributions of the ‘Resident’ and the ‘Transitional’ groups. The straight lines correspond to the best linear fits.

LCE interval ($\times 1/(10^5 yr)$)	Number of objects	Percentage with lifetimes $\geq 3Gyr$
$LCE < 0.53$	10 Objects	100%
$LCE > 0.77$	22 Objects	22%

Table 1: LCE and macroscopic stability in our sample of Trojan asteroids. It must be noted that there are no asteroids in our sample with LCE -values between $0.53 \times 1/(10^5 yr)$ and $0.77 \times 1/(10^5 yr)$.

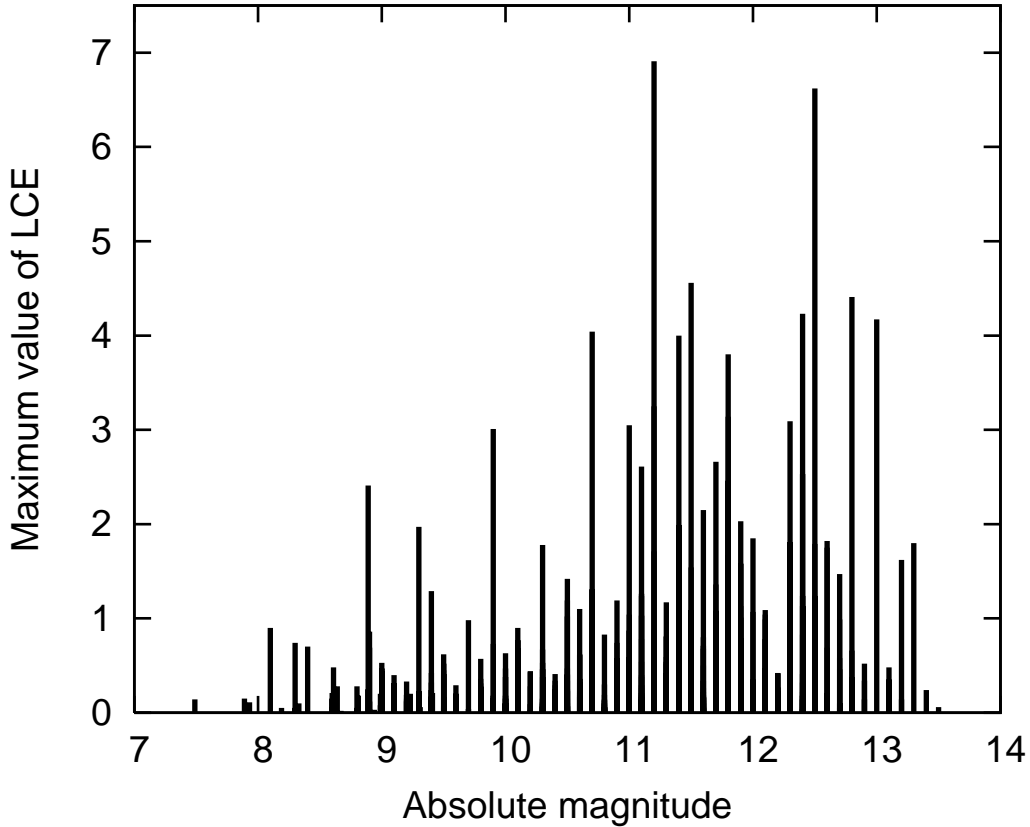


Fig. 5.— The maximum value of LCE (in units of $1/(10^5 yr)$) at a particular value of H for the numbered Trojans. It is apparent that the more unstable orbits tend to be populated by smaller objects.

Designation	Airmass	Date	UT	exp. time	N
(1173) Anchises	1.42	2005-01-08	06:51:44.502	300	3
(4754) Panthoos	1.33	2005-01-09	08:25:26.240	400	2
(11089) 1994 CS8	1.57	2005-01-08	04:40:35.215	300	4
(11273) 1988 RN11	1.58	2005-01-09	02:44:13.597	600	3
(11552) Boucolion	1.39	2005-01-10	08:14:30.182	900	2
(16560) 1991 VZ5	1.68	2005-01-09	04:38:24.950	300	3
(18137) 2000 OU30	1.42	2005-01-08	03:32:46.758	600	3
(18940) 2000 QV49	1.51	2005-01-08	05:46:04.529	900	3
(24022) 1999 RA144	1.18	2005-01-10	07:01:32.173	1200	3
(24444) 2000 OP32	1.76	2005-01-10	03:06:04.229	900	2
(32467) 2000 SL174	1.01	2005-01-08	08:05:26.299	600	3
(32615) 2001 QU277	1.58	2005-01-08	02:42:36.883	300	3
(47955) 2000 QZ73	1.44	2005-01-10	05:34:28.543	1200	3
(47957) 2000 QN116	1.50	2005-01-09	06:24:33.763	600	3
(48604) 1995 CV	1.46	2005-01-10	02:07:22.901	1200	2
“	1.50	2005-01-09	01:37:15.375	900	3
(51962) 2001 QH267	1.84	2005-01-10	03:50:52.596	900	2
(55060) 2001 QM73	1.74	2005-01-10	04:44:00.799	1200	2
(55419) 2001 TF19	1.65	2005-01-09	05:10:48.370	500	3
(68444) 2001 RH142	1.26	2005-01-09	03:48:49.472	400	3
(99306) 2001 SC101	1.56	2005-01-08	01:31:47.437	900	3

Table 2: Observational circumstances of the objects observed at NTT-ESO. The exposure time corresponds to individual images. N is the total number of images taken.

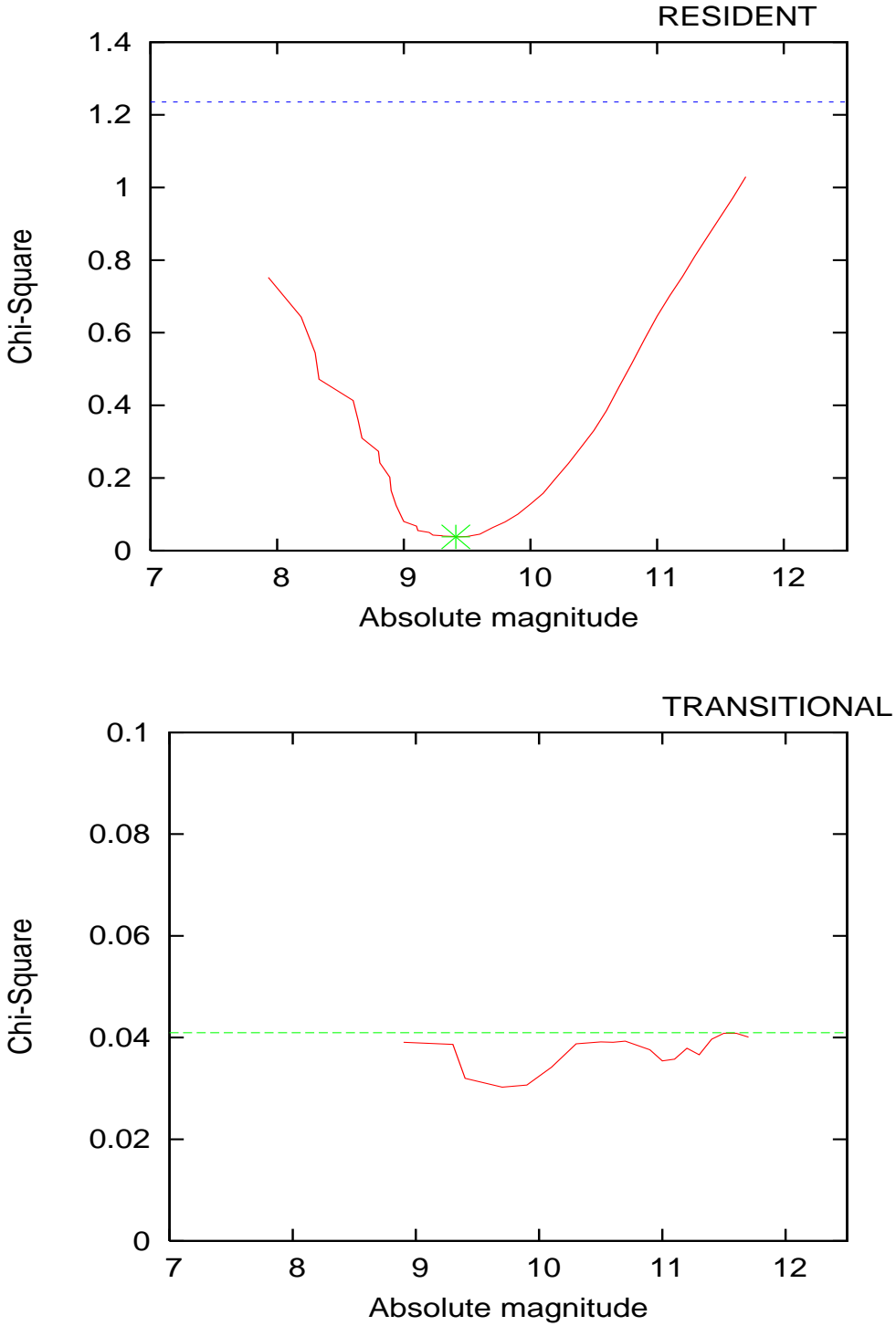


Fig. 6.— The values of χ^2 as a function of the location of the nodal point, for each group. The value of χ^2 corresponding to a fit with a single linear function from beginning to end is indicated by an horizontal line. The value of the nodal point that gives the minimum χ^2 for the resident Trojans, $H_{node} = 9.41$, is also marked. The absolute magnitude distribution

of the transitional ones. Given that the distribution of albedos in the Trojans is rather narrow (Fernandez *et al.* 2003), the size-distributions must be similar to the H distribution, therefore it is plausible that the Transitional Trojans are mainly collisional fragments. For the whole population Jewitt *et al.* 2000 also obtain a bimodal size-distribution, the nodal point is located at visual absolute magnitudes $V \approx 10$, the index for the faint branch is 0.4 and the one for the bright branch is 1.12.

4.2. Visual reflection spectra, absolute magnitude, dynamical properties and albedos

In figure 7 we plot the Absolute magnitude, H , against the normalised slope of the visible spectra, S' for all the observations. It is apparent the lack of correlation between both quantities. We have computed the linear correlation coefficient between H and S' as:

$$r_{HS'} = \frac{\sum_i^N (H_i - \overline{H})(S'_i - \overline{S'})}{\sqrt{\sum_i^N (H_i - \overline{H})^2} \sqrt{\sum_i^N (S'_i - \overline{S'})^2}},$$

where N is the total number of object with known value of S' , which is 93 in our case, \overline{H} is the mean value of H and $\overline{S'}$ is mean value of S' . The correlation coefficient between H and S' gives a value of $r_{HS'} = 0.06$, indicating that there is no correlation.

Designation	Airmass	Date	UT	exp. time (sec.)	N
(13062) Podarkes	1.48	2004-06-14	00:06	600	3
(13331) 1998 SU52	1.38	2004-06-13	21:53	900	3
(13323) 1998 SQ	1.39	2004-06-13	22:48	600	4
(15539) 2000 CN3	1.08	2004-06-13	23:49	400	3

Table 3: Observational circumstances of the objects observed at WHT-ING. The exposure time corresponds to individual images. N is the total number of images taken.

Designation	Airmass	Date	UT	exp. time (sec.)	N
(15539) 2000 CN3	1.18	2004-08-31	20:06:20	600	3
(54656) 2000 SX362	1.28	2004-08-31	19:20:02	600	3

Table 4: Observational circumstances of the objects observed at NOT. The exposure time corresponds to individual images. N is the total number of images taken.

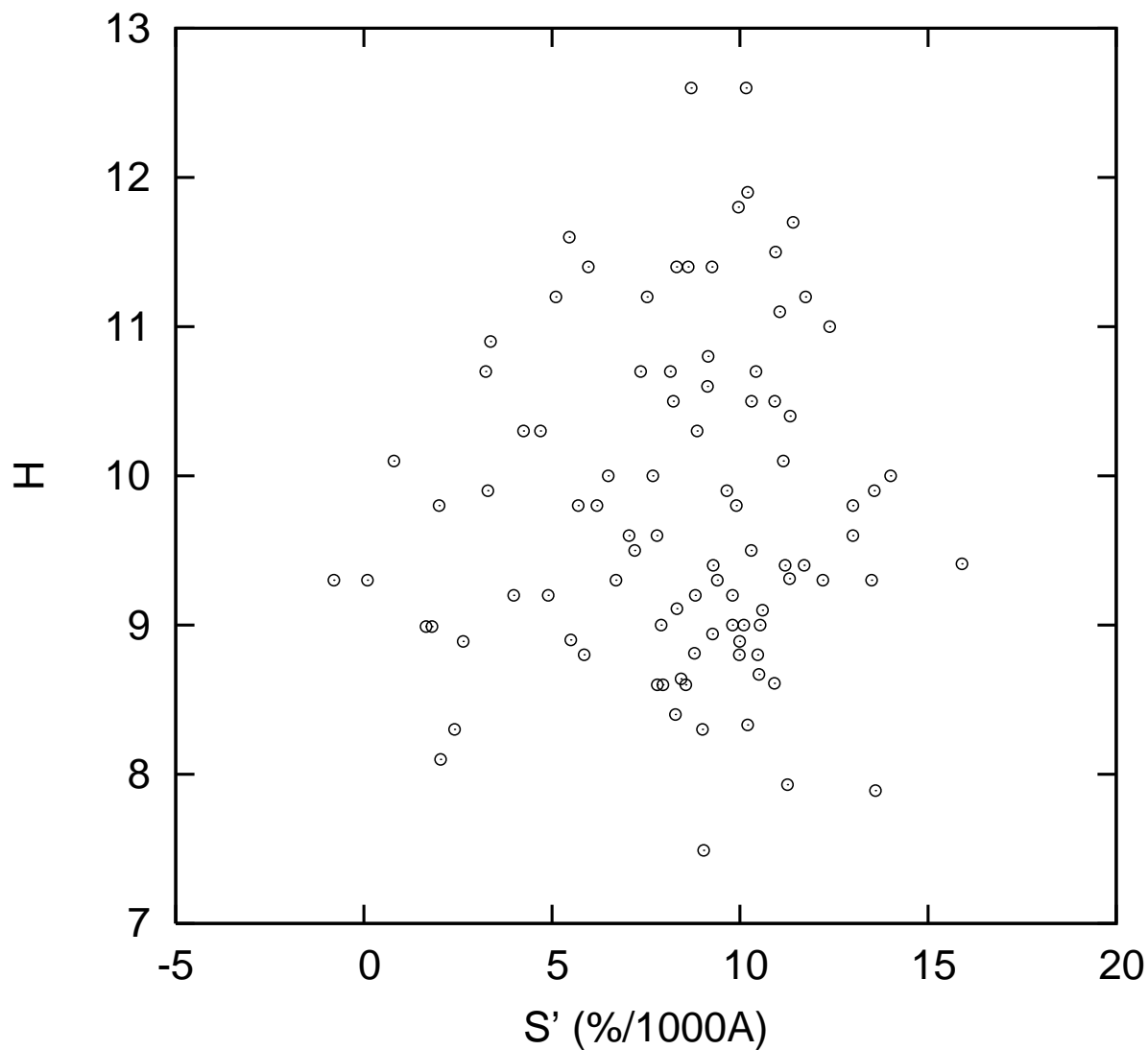


Fig. 7.— Absolute magnitude, H , vs the normalised slope of the visible spectra, S' for all the available observations.

Designation	LCE ($\times 1/(10^5 yr)$)	S' (% / 1000\AA)	$\sigma_{S'}$ (% / 1000\AA)	Swarm	H
(1173) Anchises	2.41	2.57	0.03	L5	8.89
(4754) Panthoos	0.77	11.15	0.03	L5	10.1
(11089) 1994 CS8	1.78	4.25	0.05	L5	10.3
(11273) 1988 RN11	2.15	5.46	0.06	L5	11.6
(11552) Boucolion	1.10	9.13	0.09	L5	10.6
(13062) Podarkes	2.61	11.06	0.12	L4	11.1
(13323) 1998 SQ	4.04	8.15	0.12	L4	10.7
(13331) 1998 SU52	6.91	7.53	0.20	L4	11.2
(15539) 2000 CN3 - NOT	3.01	9.65	0.13	L4	9.9
(15539) 2000 CN3 - WHT	3.01	9.69	0.10	L4	9.9
(16560) 1991 VZ5	1.19	3.37	0.04	L5	10.9
(18137) 2000 OU30	4.00	5.96	0.08	L5	11.4
(18940) 2000 QV49	1.99	8.62	0.13	L5	11.4
(24022) 1999 RA144	2.46	9.96	0.22	L5	11.8
(24444) 2000 OP32	3.25	5.11	0.15	L5	11.2
(32467) 2000 SL174	2.66	11.41	0.09	L5	11.7
(32615) 2001 QU277	1.02	8.23	0.09	L5	10.5
(47955) 2000 QZ73	1.58	10.20	0.24	L5	11.4
(47957) 2000 QN116	1.42	8.32	0.10	L5	12.6
(48604) 1995 CV	1.75	8.70	0.12	L5	10.8
(51962) 2001 QH267	0.83	9.15	0.21	L5	10.4
(54656) 2000 SX362	0.13	11.33	0.10	L5	10.7
(55060) 2001 QM73	0.97	10.42	0.16	L5	11.6
(55419) 2001 TF19	1.15	7.36	0.06	L5	10.7
(68444) 2001 RH142	1.29	11.74	0.07	L5	11.2
(99306) 2001 SC101	1.53	10.16	0.12	L5	12.6

Table 5: Dynamical stability and reflectivity gradient in our sample: values of the LCE and S' for the Trojan asteroids observed by ourselves. The corresponding Lagrangian point

Desig.	$LCE (\times 1/(10^5 yr))$	$S' (\% / 1000\text{\AA})$	$\sigma_{S'} (\% / 1000\text{\AA})$	H (mag)	Swarm	Ref. id.
588	0.02	10.50	0.20	8.7	L4	3
624	0.14	9.03	0.05	7.5	L4	1
659	0.20	1.66	0.16	9.0	L4	1
884	0.18	8.79	0.10	8.8	L5	1
911	0.15	13.60	0.10	7.9	L4	3
1143	0.11	11.26	0.33	7.9	L4	2
1172	0.10	12.30	0.10	8.3	L5	3
1172	0.10	8.11	0.09	8.33	L5	1
1173	2.41	2.72	0.08	8.9	L5	1
1208	0.08	1.81	0.14	9.0	L5	1
1437	0.74	2.41	0.07	8.3	L4	1
1583	0.06	8.56	0.09	8.6	L4	1
1647	0.07	8.86	0.35	10.3	L4	1
1749	0.19	8.62	0.10	9.2	L4	1
1749	0.19	9.01	0.26	9.2	L4	2
1867	0.48	10.91	0.09	8.6	L5	1
1868	1.97	6.70	0.10	9.3	L4	3
1870	0.03	20.34	0.48	10.5	L5	1
1871	0.51	12.38	0.89	11.0	L5	1
1872	0.20	25.42	1.15	11.2	L5	1
1873	0.25	10.30	0.36	10.5	L5	1
2207	0.25	9.99	0.12	9.0	L5	1
2223	0.21	15.90	0.10	9.4	L5	3
2241	0.28	8.43	0.11	8.6	L5	1
2260	0.06	11.32	0.26	9.3	L4	1
2357	0.03	9.27	0.12	8.9	L5	1
2363	0.01	8.32	0.21	9.1	L5	1
2456	0.29	7.79	0.11	9.6	L4	1
2674	0.12	10.54	0.15	9.0	L5	1

Desig.	LCE ($\times 1/(10^5 yr)$)	S' (% / 1000\AA)	$\sigma_{S'}$ (% / 1000\AA)	H (mag)	Swarm	Ref. id.
2759	0.08	9.90	0.16	9.8	L4	1
2797	0.70	8.28	0.07	8.4	L4	1
2895	0.05	0.10	0.60	9.3	L5	3
2920	0.28	10.17	0.21	8.8	L4	2
2920	0.28	9.80	0.08	8.8	L4	1
3063	0.21	7.95	0.05	8.6	L4	4
3240	0.03	7.68	0.31	10.0	L5	1
3317	0.05	10.47	0.04	8.3	L5	3
3317	0.05	7.54	0.12	8.3	L5	2
3391	0.38	4.69	0.31	10.3	L4	1
3451	0.90	1.89	0.10	8.1	L5	2
3451	0.90	2.24	0.09	8.1	L5	1
3708	0.03	9.40	0.10	9.3	L5	3
3709	0.04	10.95	0.07	9.0	L4	4
3709	0.04	8.40	0.10	9.0	L4	3
3793	0.01	3.66	0.13	8.8	L4	1
3793	0.01	7.44	0.07	8.8	L4	4
4035	0.11	15.45	0.05	9.3	L4	5
4035	0.11	8.80	0.10	9.3	L4	3
4060	0.12	5.50	0.10	8.9	L4	3
4063	0.15	6.64	0.04	8.6	L4	4
4063	0.15	8.40	0.10	8.6	L4	3
4068	0.42	10.27	0.04	9.4	L4	4
4068	0.42	10.30	0.14	9.4	L4	1
4068	0.42	14.40	0.10	9.4	L4	3
4138	0.07	2.00	0.20	9.8	L4	3
4348	0.13	3.98	0.04	9.2	L5	3
4489	0.53	7.90	0.09	9.0	L4	4
4715	0.15	13.50	0.20	9.3	L5	3

Desig.	$LCE (\times 1/(10^5 yr))$	$S' (\% / 1000\text{\AA})$	$\sigma_{S'} (\% / 1000\text{\AA})$	H (mag)	Swarm	Ref. id.
4792	0.10	14.00	0.20	10.0	L5	3
4833	0.31	10.04	0.09	9.1	L4	4
4833	0.31	11.20	0.10	9.1	L4	3
4834	0.12	9.80	0.10	9.2	L4	3
4835	0.16	5.00	0.20	9.8	L4	3
4835	0.16	7.96	0.07	9.8	L4	4
4836	0.16	7.20	0.10	9.5	L4	3
4902	0.05	7.05	0.07	9.6	L4	4
5025	0.07	13.00	0.30	9.8	L4	3
5027	0.17	9.29	0.32	9.4	L4	1
5028	0.15	13.57	0.39	9.9	L4	1
5126	0.08	0.80	0.10	10.1	L4	3
5254	0.05	10.47	0.04	8.8	L4	3
5258	0.18	6.50	0.30	10.0	L4	3
5264	0.01	11.50	0.20	9.5	L4	3
5264	0.01	8.77	0.09	9.5	L4	4
5283	0.07	-8.90	0.10	9.3	L4	3
5285	0.31	5.70	0.10	9.8	L4	3
5511	0.13	13.00	0.10	9.6	L5	3
5648	0.33	4.90	0.40	9.0	L5	3
6090	0.32	11.70	0.20	9.4	L4	3
7152	0.07	3.30	0.20	9.9	L4	3
7352	0.47	9.80	0.20	9.0	L5	3
7641	0.02	-0.80	0.20	9.3	L4	3
11351	0.40	10.92	0.13	10.5	L4	5
12921	0.08	3.24	0.08	10.7	L4	5
20738	0.06	9.25	0.15	11.4	L4	5
24341	0.44	10.94	0.09	11.5	L4	5

Table 2: Data for the fourth TESS transit detected for the star labeled III.

Designation	$ \Delta S' $	Between	
1172	4.19	Jewitt	Bendoya
1173	0.14	Jewitt	NTT-ESO
1749	0.39	Jewitt	SMASSII
2920	0.37	Jewitt	SMASSII
3317	2.93	Bendoya	SMASSII
3451	0.35	SMASSII	Jewitt
3709	2.55	Bendoya	Lazzaro
3793	3.77	Jewitt	Lazzaro
4035	6.65	Bendoya	Dotto
4063	1.76	Bendoya	Lazzaro
4068	4.13	Bendoya	Lazzaro
4068	4.10	Bendoya	Jewitt
4068	0.04	Jewitt	Lazzaro
4833	1.16	Bendoya	Lazzaro
4835	2.96	Bendoya	Lazzaro
5264	2.73	Bendoya	Lazzaro
15539	0.04	WHT-ING	NOT

Table 9: Magnitudes of the differences in S' , $|\Delta S'|$, for objects repeated in the available sample.

In Figure 8, we plot LCE against S' . A correlation between the dynamical stability and the visible color is not apparent, and the distributions of slopes of both the transitional and the resident groups have a similar wide range. As in section 4.1, we divide this sample into 2 groups, the *resident* Trojans have $LCE_{res} \leq 0.53 \times 1/(10^5 yr)$, comprising 65 objects and the *transitional* ones, $LCE_{trans} > 0.53 \times 1/(10^5 yr)$, with 28 objects.

The probability, p_{KS} , that the samples of visible colors, corresponding to the unstable and the stable groups, are drawn from the same distribution, given by a Kolmogorov-Smirnov test, is very small: $p_{KS} = 0.17$. This result is probably due to the small size of the sample. The median value, $\langle S' \rangle_{med}$, corresponding to the transitional objects is slightly more neutral than the one corresponding to the residents (see table 11), although both values are similar within the error bounds. If we divide the sample according to the value of LCE into more than 2 groups, there is a weak tendency for the more stable objects to be redder (see figure 9).

A slight excess of neutral objects exists in the transitional group (see figure 10). As we have discussed in section 4.1, transitional Trojans can be associated with collisional by-products, which are expected to have younger surfaces. This result might indicate that Trojan young surfaces are neutral and they tend to redden with age.

Group	b	χ^2
Big resident ($H < 9.41$)	0.89	0.037
Small resident ($H \geq 9.41$)	0.37	
Transitional	0.45	0.041

Table 10: Slopes of the linear fits of the size distribution of the Resident (Big and Small) and Transitional groups. Notice that the value of χ^2 for the resident group corresponds to a single bimodal fit.

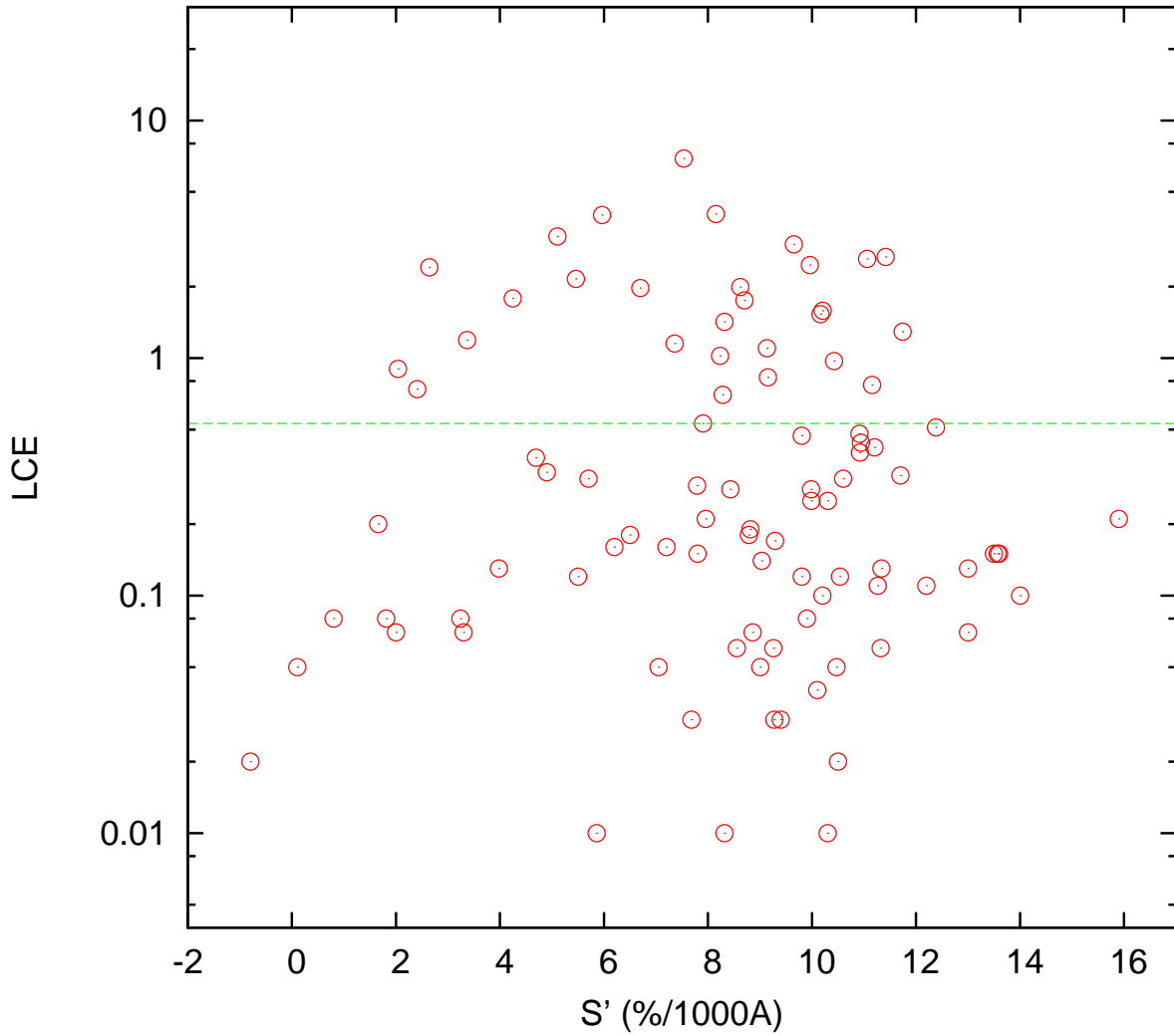


Fig. 8.— Lyapunov characteristic exponent, LCE (in $1/(10^5 yr)$ units), as a function of the slope of the visible spectra, $\langle S' \rangle$ for the Trojan asteroids. Objects above the horizontal line are considered transitional while the ones below the line are considered resident.

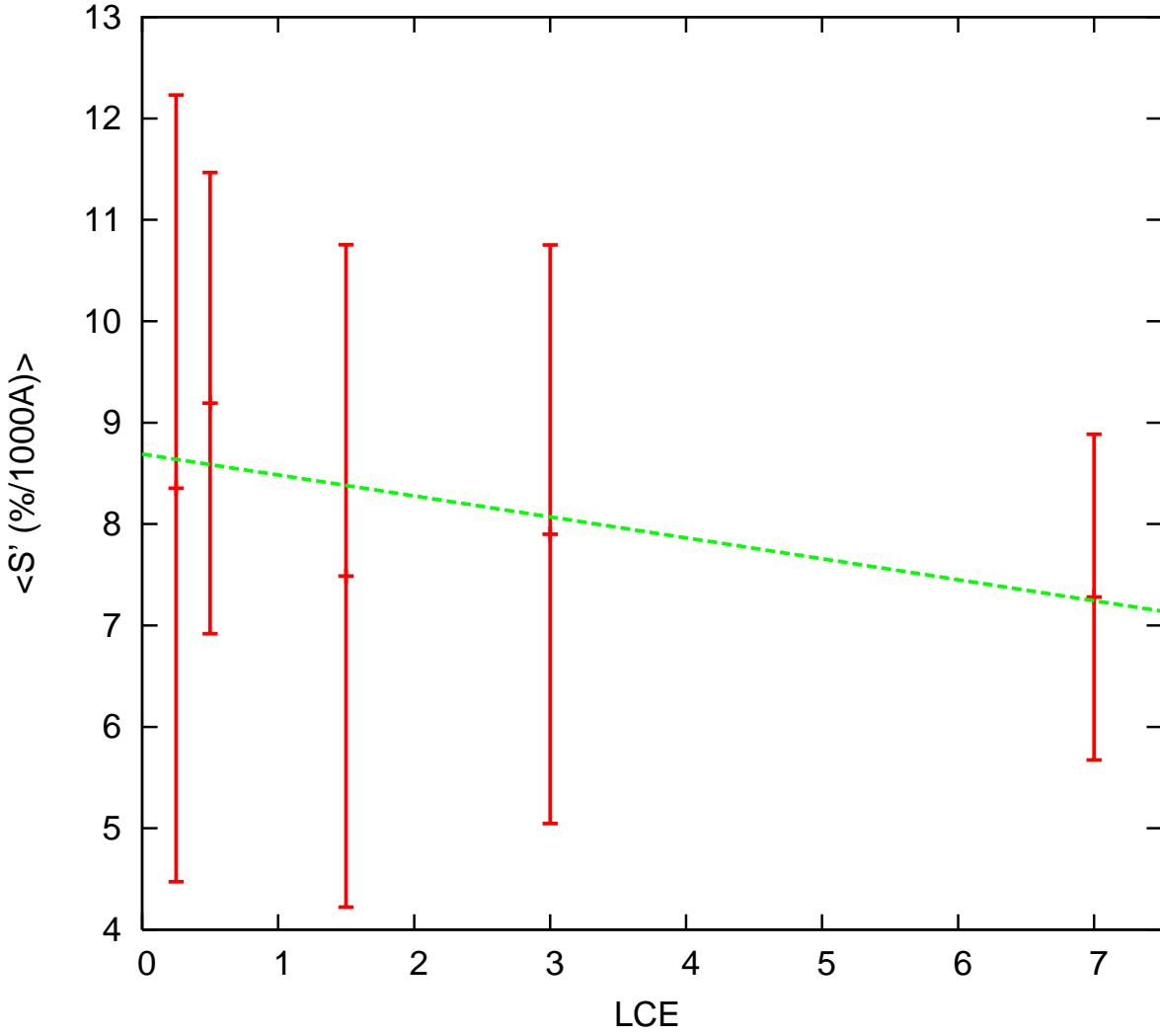


Fig. 9.— Mean value of the slope of the visible spectra, $\langle S' \rangle$ as a function of LCE (in $1/(10^5 yr)$ units). The corresponding dispersions are indicated by the error bars. The straight line corresponds to a minimum-squares linear fit.

Group	$\langle S' \rangle_{med}$ ($\%/1000\text{\AA}$)	$\sigma_{S'}$ ($\%/1000\text{\AA}$)
Resident	9.18	3.22
Transitional	8.18	2.63

Table 11: Median value of the slope of the visible spectra, $\langle S' \rangle$ and its dispersion, $\sigma_{S'}$, for the Resident and the Transitional groups.

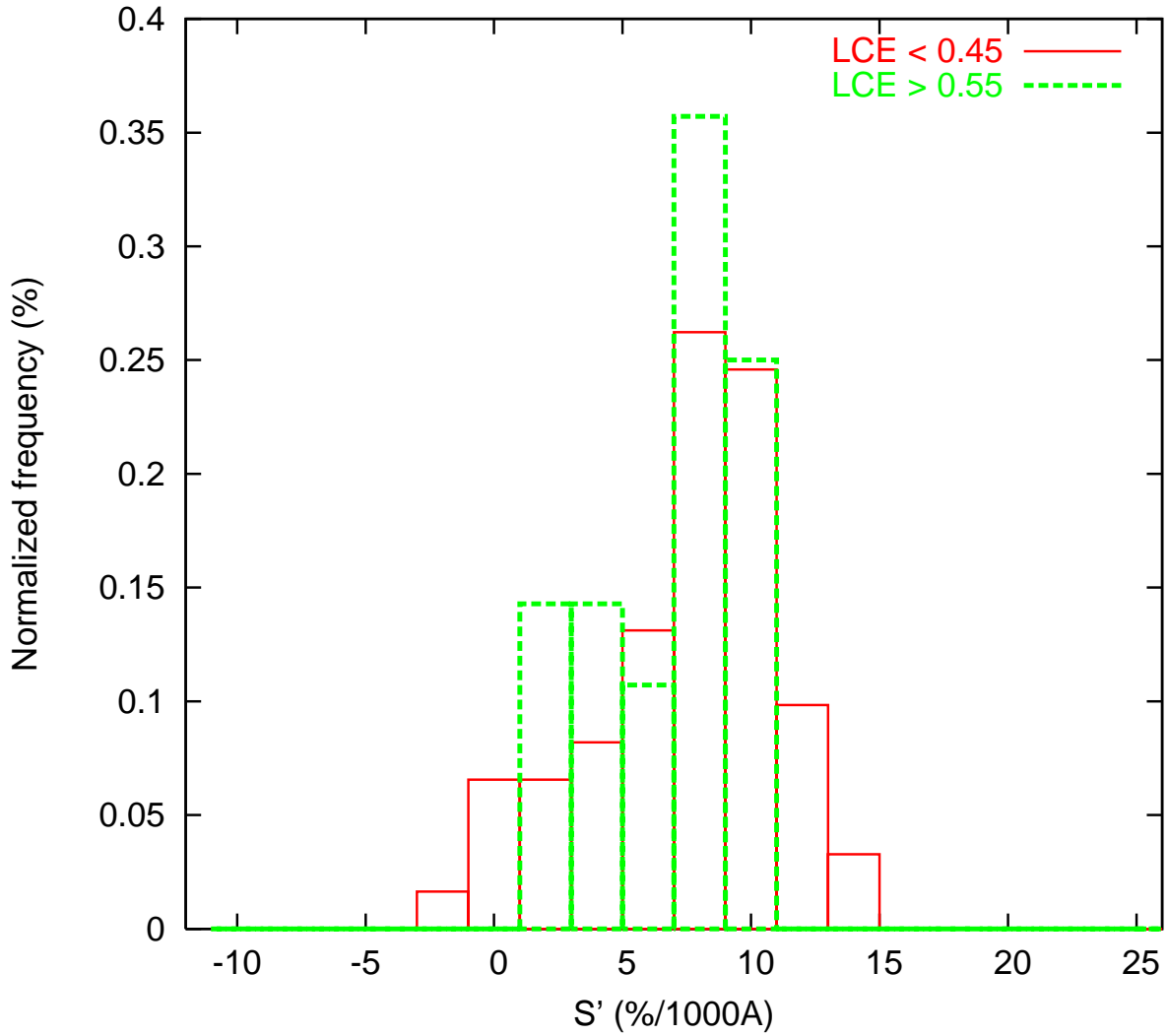


Fig. 10.— Histograms of S' for both the Resident and the Transitional groups.

To study correlations between albedo and color or orbital stability, we used the IRAS geometrical albedos (Tedesco *et al.* 2002) and those obtained by Fernández *et al.* (2003), corresponding to the 48 Trojan asteroids that were in our spectroscopic sample. We did not find any apparent relationship between those parameters.

We did not find either any statistical differences in the samples of S' , corresponding to the L4 and L5 clouds, composed of 50 and 43 objects respectively (see Table 12).

5. Discussion

Before performing the observation presented here, we found only 4 Trojan asteroids with determined visual spectra in orbits with $LCE > 0.53 \times 1/(10^5 yr)$ (see tables 6, 7 and 8). Therefore, our data has increased by a factor of five the number of measured visible-spectra of Trojans on unstable orbits. Using this increased sample, we have studied the distribution of visible-spectroscopic observations of the Trojan asteroids and search for correlations with orbital stability, size and albedo.

Some physical characteristics, such as the size distribution, are expected to be related with orbital stability, due to energy equipartition after a physical collision. We find that, while the absolute-magnitude distribution of the Trojans in stable orbits is bimodal, the one corresponding to the unstable orbits is unimodal, with a slope similar to the one for

Cloud	$\langle S' \rangle_{med}$	$\sigma_{S'}$	N
L4	7.82	3.54	47
L5	7.58	3.60	46

Table 12: Median value of the slope of the visible spectra, $\langle S' \rangle_{med}$ and its dispersion, $\sigma_{S'}$, and the size of each sample, N , for the L4 and L5 clouds.

the small stable Trojans. Given the location of the node for the bimodal distribution of the stable objects and the smallest absolute magnitude of the transitional ones, we deduce that fragments of collision become more abundant at $H \gtrsim 9.4$. On the other hand, we find no correlation between size and spectral slope. The resident and the transitional (smaller) objects, do not differ statistically in their surface properties. Therefore, we conclude that the collisional process that feeds the unstable orbits and creates smaller bodies is not altering noticeably the distribution of surface properties.

References

- Brunetto, R., Barucci, M. A., Dotto, E. and Strazzulla, G. 2006a. Ion Irradiation of Frozen Methanol, Methane, and Benzene: Linking to the Colors of Centaurs and Trans-Neptunian Objects. *The Astrophysical Journal*, **644**, 1, 646-650.
- Brunetto, R., Romano, F., Blanco, A., Fonti, S., Martino, M., Orofino, V., Verrienti, C. 2006b. Space weathering of silicates simulated by nanosecond pulse UV excimer laser. *Icarus*, **180**, 2, 546-554. y
- Bus, S.J. 1999. Compositional structure in the asteroid belt: results of a spectroscopic survey. *PhD Thesis*, MIT, Cambridge.
- Bendjoya.,P, Cellino, A, Di Martino, M. and Saba, L. 2004. Spectroscopic observations of Jupiter Trojans. *Icarus*, **168**, 2, 374-384.
- Chambers, J.E. 1999. A Hybrid Symplectic Integrator that Permits Close Encounters between Massive Bodies. *M.N.R.A.S.*, **304**, 793-799.
- Cruikshank, D. P., Dalle Ore, C. M., Roush, T. L., Geballe, T. R., Owen, T. C., de Bergh, C., Cash, M. D.; Hartmann, W. K. 2001. Constraints on the Composition of Trojan

Asteroid 624 Hektor. *Icarus*, **153**, Issue 2, 348-360.

Dell’Oro, A., Marzari, P., Paolicchi F., Dotto, E., Vanzani, V. 1998. Trojan collision probability: a statistical approach. *Astronomy and Astrophysics*, **339**, 272-277.

Dotto, E., Fornasier, S., Barucci, M. A., Licandro, J., Boehnhardt, H., Hainaut, O., Marzari, F., De Bergh, C., De Luise, F. 2006. The surface composition of Jupiter Trojans: Visible and Infrared survey of dynamical Families. *Icarus*, **183**, 2, 420-434.

Dvorack, R., Tsiganis, K. 2000. Why do Trojan ASCS (not) escape?. *Celestial Mechanics and Dynamical Astronomy*, **78**, 125-136.

Emery, J. P. and Brown, R. H. 2003. Constraints on the surface composition of Trojan asteroids from near-infrared (0.8-4.0 μ) spectroscopy *Icarus*, **164**, 1, 104-121.

Emery, J. P. and Brown, R. H. 2004. The surface composition of Trojan asteroids: constraints set by scattering theory. *Icarus*, **170**, 1, 131-152.

Emery J.P., Cruikshank D.P. and Van Cleve J. 2006. Thermal emission spectroscopy (5.2-38 μ) of three Trojan asteroids with the Spitzer Space Telescope: Detection of fine-grained silicates. *Icarus*, **82**, 2, 496-512.

Fernández, Y. R. and Sheppard, S. S. and Jewitt, D. C. 2003. The Albedo Distribution of Jovian Trojan Asteroids. *The Astronomical Journal*, **126**, 1563-1574.

Fornasier, S., Dotto, E., Marzari, F., Barucci, M. A., Boehnhardt, H. and Hainaut, O. and de Bergh, C., 2004, Visible spectroscopic and photometric survey of L5 Trojans: investigation of dynamical families, *Icarus*, **172**, 221-232.

Fornasier, S., Dotto E., Hainaut O., Marzari, F., Boehnhardt, H., De Luise F. and Barucci M.A. 2007, Visible spectroscopic and photometric survey of Jupiter Trojans: Final result on dynamical families, *Icarus*, **190**, 622-642.

Gil-Hutton, R. 2002. Color diversity among Kuiper belt objects: The collisional resurfacing model revisited. *Planetary and Space Science*, **50**, 1, 57-62.

Holsapple K.A. 1993. The scaling of impact processes in planetary sciences. *Annu. Rev. Earth Planet. Sci.*, **21**, 333-374.

Horner J, Evans N.W. and Bailey M.E. 2005. Simulation of the Population of Centaurs II. Individual objects. *M.N.R.A.S.*, **355**, 2, 321-329.

Jewitt, D.C. 2002, From Kuiper Belt Object to Cometary Nucleus: The Missing Ultrared Matter. *The Astronomical Journal*, **123**, 2, 1039-1049.

Jewitt, David C., Luu, Jane X. 1990. CCD spectra of asteroids. II - The Trojans as spectral analogs of cometary nuclei. *Astronomical Journal*, **100**, 933-944.

Jewitt, David C., Trujillo, Chadwick A., Luu, Jane X. 2000. Population and Size Distribution of Small Jovian Trojan Asteroids. *The Astronomical Journal*, **120**, 2, 1140-1147.

Karlsson, O. 2004. Transitional and temporary objects in the Jupiter Trojan area. *Astronomy and Astrophysics*, **413**, 1153-1161.

Landolt, A. U. 1992. UBVRI photometric standard stars in the magnitude range 11.5-16.0 around the celestial equator. *Astr. J.* **104**, 1, 340-371, 436-491.

Lazzaro, D., Angeli, C. A., Carvano, J. M., Mothe-Diniz, T.; Duffard, R.; Florczak, M. 2004. S3OS2: The visible spectroscopic survey of 820 asteroids. *Icarus*, **172**, 179–220.

Levison, H., Shoemaker, E. M., Shoemaker, C. S. 1997. The dispersal of the Trojan asteroid swarm. *Nature*, **385**, 42-44.

Marzari, F., Farinella, P., Vanzani, V. Are Trojan collisional families a source for short-period comets?. 1995. *Astronomy and Astrophysics*, **299**, 267.

Marzari, F. and Scholl, H. 1998. Capture of Trojans by a Growing Proto-Jupiter *Icarus*, **131**, 1, 41-51.

Milani, A., Nobili, A.M. 1992. An example of stable chaos in the Solar System *Nature*. **357**, 6379, 569-571.

Milani, A. 1993. The Trojan asteroid belt: Proper elements, stability, chaos and families *Celestial Mechanics and Dynamical Astronomy*, **57**, 1-2, 59-94.

Milani, A., Nobili, A.M., Knezevic, Z. 1997. Stable Chaos in the Asteroid Belt. *Icarus*, **125**, 1, 13-31.

Morbidelli, A., Levison, H. F., Tsiganis, K. and Gomes, R. 2005. Chaotic capture of Jupiter's Trojan asteroids in the early Solar System *Nature*, **435**, 7041, 462-465.

Moroz, L., Baratta, G., Strazzulla, G., Starukhina, L., Dotto, E., Barucci, M.A., Arnold, G., Distefano, E. 2004. *Icarus*, **170**, 1, 214-228.

Nesvorny, D. and Dones, L. 2002. How Long-Lived Are the Hypothetical Trojan Populations of Saturn, Uranus, and Neptune? *Icarus*, **160**, 2, 271-288.

Petit, J.M. and Farinella, P. 1993. Modelling the outcomes of high-velocity impacts between small solar system bodies. *Celestial Mechanics and Dynamical Astronomy*, **57**, 1-2, 1-28.

Pilat-Lohinger, E., Dvorak, R. 1999. Trojans in Stable Chaotic Motion. *Celestial Mechanics and Dynamical Astronomy*, **73**, 117-126.

Rabe, E. 1972. Orbital Characteristics of Comets Passing Through the 1:1 Commensurability with Jupiter. The Motion, Evolution of Orbits, and Origin of Comets, Proceedings from IAU Symposium no. 45, held in Leningrad, U.S.S.R., August 4-11, 1970. Edited by Gleb Aleksandrovich Chebotarev, E. I. Kazimirchak-Polonskaia, and B. G.

Marsden. International Astronomical Union. Symposium no. 45, Dordrecht, Reidel, p.55.

Strazzulla, G., Dotto, E., Binzel, R., Brunetto, R., Barucci, M. A., Blanco, A., Orofino, V. 2005. Spectral alteration of the Meteorite Epinal (H5) induced by heavy ion irradiation: a simulation of space weathering effects on near-Earth asteroids. *Icarus*, **174**, 1, 31-35.

Tedesco, E.F., Noah, P.V., Noah, M., Price and Stephan D. 2002. The Supplemental IRAS Minor Planet Survey. *The Astronomical Journal*, **123**, 2, 1056-1085.

Tsiganis, K., Dvorak, R., Pilat-Lohinger, E. 2000. Thersites: a jumping' Trojan? *Astronomy and Astrophysics*, **354**, 1091-1100.

Tsiganis, K., Varvoglis, H., Dvorak, R. 2005. Chaotic Diffusion And Effective Stability of Jupiter Trojans *Celestial Mechanics and Dynamical Astronomy*, **92**, 1-3. 71-87

Yang, B, Jewitt, D. 2007. Spectroscopic Search for Water Ice on Jovian Trojan Asteroids. *The Astronomical Journal*, **134**, 1, 223-228.

Yoder, C. F. 1979. Notes on the origin of the Trojan asteroids. *Icarus*, **40**, 341-344.